



HAL
open science

Mechanistic modeling of the dynamics of phage attack during milk acidification in the cheese-making process

Michèle Bou Habib, Emmanuel Bernuau, Benjamín-José Sánchez, Dominique Swennen, Ahmad A. Zeidan, Cristian Trelea, Jannik Vindeloev

► **To cite this version:**

Michèle Bou Habib, Emmanuel Bernuau, Benjamín-José Sánchez, Dominique Swennen, Ahmad A. Zeidan, et al.. Mechanistic modeling of the dynamics of phage attack during milk acidification in the cheese-making process. *Journal of Food Engineering*, 2025, 387, pp.112329. 10.1016/j.jfoodeng.2024.112329 . hal-04741360

HAL Id: hal-04741360

<https://hal.science/hal-04741360v1>

Submitted on 17 Oct 2024

HAL is a multi-disciplinary open access archive for the deposit and dissemination of scientific research documents, whether they are published or not. The documents may come from teaching and research institutions in France or abroad, or from public or private research centers.

L'archive ouverte pluridisciplinaire **HAL**, est destinée au dépôt et à la diffusion de documents scientifiques de niveau recherche, publiés ou non, émanant des établissements d'enseignement et de recherche français ou étrangers, des laboratoires publics ou privés.



Distributed under a Creative Commons Attribution 4.0 International License

1 Highlights

2 **Mechanistic modeling of the dynamics of phage attack during milk acidification in the cheese-** 3 **making process**

4 Michèle Bou Habib, Emmanuel Bernuau, Benjamín José Sánchez, Dominique Swennen, Ahmad A. Zeidan, Ioan-Cristian
5 Trelea, Jannik Vindelov

- 6 • Prediction of success/failure of milk acidification in the presence of phage
- 7 • Development and experimental validation of a dynamic mechanistic model
- 8 • Identification of key interactions to enhance phage attack interventions

Mechanistic modeling of the dynamics of phage attack during milk acidification in the cheese-making process

Michèle Bou Habib^a, Emmanuel Bernuau^{a,*}, Benjamín José Sánchez^b, Dominique Swennen^a, Ahmad A. Zeidan^b, Ioan-Cristian Trelea^a and Jannik Vindelov^b

^aUniversité Paris-Saclay, INRAE, AgroParisTech, UMR SayFood, Palaiseau, 91120, France

^bNovonosis, R&D, Hørsholm, 2970, Denmark

ARTICLE INFO

Keywords:
kinetic model
virulent phage
Lactococcus lactis
model validation

ABSTRACT


Bacteriophage attacks represent a major threat in the dairy industry. Here, an unstructured mechanistic model predicting the dynamics of milk acidification in case of phage attack was developed and experimentally validated. Multiple acidification experiments were run with different combinations of initial phage titers and bacterial concentrations and the resulting *pH* dynamics were recorded. The model could successfully predict the success or failure of milk acidification. Using the model, important biological parameters were deduced from simple, low-cost acidification measurements. These parameters included bacteria's maximum growth and lysis rates, phages' burst size, etc. Sensitivity analysis helped identify biologically relevant aspects of phage-host interactions. Growth and lysis kinetics were shown to have the most important impacts. This knowledge can be used to develop easy routine strategies to fight phage attack in the dairy industry. The model can be used to raise awareness amongst cheese makers on the importance of cleaning to avoid food and material waste.

1. Introduction

Microorganisms play a crucial role in cheese production, both during the acidification and ripening steps (Marcó et al., 2012). During the former, lactic acid bacteria (LAB), such as *Streptococcus thermophilus*, *Lactococcus lactis*, and *Lactococcus cremoris*, are used to convert lactose to lactic acid, thus acidifying milk. This step largely impacts the final cheese composition and quality (Kongo, 2013). To control the fermentation and obtain high-quality end-products, an inoculation in the order of 10^7 Colony Forming Units per mL (CFU/mL) of milk is typically required (Garneau and Moineau, 2011).

According to Moineau and Lévesque (2005), between 0.1% and 10% of industrial milk fermentations are negatively affected by bacteriophages (or phages), i.e., viruses that attack bacteria. In milk fermentation, phages slow down or even completely inhibit LAB growth, therefore preventing milk acidification. It is a common practice in dairies to use the same cheese vat repeatedly, with only limited cleaning or rinsing between fillings. The LAB culture is added during the filling of the cheese vat with milk to save time and better distribute the cells. After a set fermentation time, the content of the vat is emptied and processed further downstream Fox and McSweeney (2017). The vat is considered ready for another filling round after a quick rinse. During these successive fillings, phages may build up and cause fermentation failure. Whenever the fermentation is halted in this way, significant economic losses and environmental

*Corresponding author

 emmanuel.bernuau@agroparistech.fr (E. Bernuau)

47 issues arise, as milk is discarded and the plant needs to be thoroughly cleaned (Brüssow, 2001). In less drastic cases,
48 the production is slowed down, resulting in reduced cheese quality and longer production times (Ledebøer et al., 2002).

49 As shown in Figure 1, there are two types of phage attack cycles: the lytic and the lysogenic cycles. Virulent phages
50 undergo exclusively lytic cycles, whereas temperate phages can undergo both cycles.

51 In the beginning of both cycles, the phage is adsorbed on the surface of the host bacterium. Afterward, the phage
52 injects its genetic material into the bacterium. In the case of a lytic cycle, the phage's genome is replicated inside the
53 bacterial cell, and after some time, known as the latency time, the infected cell is lysed and releases the newly created
54 phages in a sudden burst. The released progeny is then ready to infect new cells, and the cycle is repeated. In the case
55 of a lysogenic cycle, the phage's genome is integrated inside the bacteria's chromosome and forms what is known as a
56 "prophage." The phage's genome stays and replicates within the bacteria's chromosome for multiple generations until
57 the prophage enters the lytic cycle due to environmental stresses (Sinha et al., 2020). Most lactococcal phages found
58 in failed industrial milk fermentations belong to either of three groups: the 936 and c2 phage groups, which are all
59 virulent, and the P335 phage group, whose phages can be either temperate or virulent (Mahony et al., 2015).

60 Simulations are a valuable tool to gain deeper insight into the dynamics of phage attack (Santos et al., 2014).
61 One approach is to use dynamic, unstructured mechanistic models, as they do not only simulate a process' temporal
62 evolution but also help better understand the physical, chemical, and biological phenomena involved. On the one hand,
63 this is accomplished by selecting the model structure that fits the experimental data best. On the other hand, the study
64 of the model's sensitivity to parameter variations gives an indication of the most influential phenomena.

65 Campbell (1961) was the first to propose a model to describe the dynamics of phage attack. The model consisted of
66 two differential equations describing the evolution of bacteria and phages. It included mechanisms for bacterial growth,
67 phage adsorption, phage inactivation, and burst of progeny while considering the latency time between bacterial
68 infection and lysis. This model was a starting point from which several other models have been derived by changing
69 the expression of some terms or studying in more detail some mechanisms (Santos et al., 2014; Chaudhry et al., 2018;
70 Beretta and Kuang, 1998; Bull et al., 2006; Levin et al., 1977). Key biological parameters such as adsorption rate,
71 latent period, burst size, bacterial growth rate, and substrate uptake rate are common to all these models. Levin et al.
72 (1977) proposed a generalized model to describe any number of species of susceptible bacteria. They modeled infected
73 bacteria, growth-limiting substrates, and phages as well. Beretta and Kuang (1998) proposed a model where susceptible
74 bacteria reproduce while infected bacteria are removed by lysis. A new parameter, lysis or death rate, was introduced.
75 It is the inverse of the latent period and indicates the number of cells lysed per unit time. Finally, in some studies,
76 models have been extended to include acquired bacterial resistance to phages (Santos et al., 2014; Chaudhry et al.,
77 2018; Lenski and Levin, 1985; Cairns et al., 2009).

78 Among the few published phage attack models, most are in the field of phage therapy and disease epidemics;
79 models applied to the fields of food science, wastewater, and bioremediation are still lacking. Additionally, only a few
80 of the developed models have been validated experimentally. Among these experimentally validated models, such as
81 Santos et al. (2014) and Levin et al. (1977), experiments were conducted under only one specific set of conditions
82 and in only one replicate. Finally, the applicability to a range of practical situations and the robustness to variations in
83 experimental conditions were not investigated.

84 The objective of this work was to develop and validate an unstructured mechanistic model to predict milk
85 acidification by *Lactococcus lactis*, a key player in cheese fermentation, in the presence of a virulent phage.

86 In this paper, we start by explaining the experimental setup in Section 2. In Section 3, we show the experimental
87 acidification results. We then detail, in Section 4, the model development based on these experiments. Then, in Section
88 5, we focus on estimating key biologically meaningful parameters. Finally, we conclude in Section 6.

89 2. Experimental Setup

90 2.1. Strains and milk

91 One *Lactococcus lactis* strain (strain A) and one *Cedrovirus Lactococcus* phage c2 (phage B), both obtained from
92 the Chr. Hansen Culture Collection, were used to model phage-host dynamics. In this experimental setup, the bacterial
93 strain was maintained as a frozen pellets at -20°C (or lower), while a phage stock was kept at 4°C after preparation of
94 the lysate (Poulsen et al., 2019). Milk acidification experiments were carried out using B-milk, which is prepared using
95 low-fat skim milk powder to a level of dry matter of 9.5% and subjected to heating at 99°C for 30 min, followed by
96 cooling at 30°C. The milk was kept at 4°C until further use. B-milk was then supplemented with 50 mg of bromocresol
97 purple salt and 50 mg of bromocresol green salt (both from Sigma Aldrich, St. Louis, Missouri, United States) as a *pH*
98 color indicator, as previously described (Poulsen et al., 2019).

99 2.2. Experimental design and *pH* measurements

100 Acidification experiments were performed in a volume of 400µL using deep 96-well plates, and a 2D concentration-
101 gradient of strain-to-phage was prepared using a Hamilton MicroLab platform (Hamilton, Bonaduz, Switzerland). The
102 sensitive strain was supplied in frozen pellets to concentrations ranging from 10g/100L of dry weight ($\sim 10^6$ CFU/mL)
103 to 80g/100L ($\sim 8.0 \times 10^6$ CFU/mL), while the phage concentrations varied between 0 and 10^7 Plaque Forming Units
104 per mL (PFU/mL).

105 After inoculation of the sensitive strain and its phage, the plates were incubated for 20h on top of a flat-bed scanner
106 (HP ScanJet G4010) at 30°C (mesophilic culture). *pH*-dependent changes in color were recorded every 4 min and
107 converted into *pH* values using *pH* Coprah software (v.2.1.52; Videometer, Copenhagen, Denmark).

108 The data consisted of 2 separate runs, with 3 replicates for each run, for 48 acidification curves with 12 different
 109 initial phage (P_0) titers and 4 different initial susceptible bacteria (X_{s0}) concentrations in 3 replicates. The experiment
 110 is summarized in a conceptual diagram in Figure 2.

111 3. Experimental Acidification Data

112 Figure 3 shows an example of available data of runs Run_01 and Run_02 for an initial bacteria concentration of
 113 40 g/100L and an initial phage titer of 0.

114 After inoculation, bacteria require time, known as lag time, to adapt to a new environment. Afterward, acidification
 115 starts. The initial pH of milk is 6.6. A steep decrease in pH indicates fast acidification for the first 4 hours where pH
 116 reached a value of 4.6. The acidification then slows down until it completely stops towards the end of the experiment.
 117 The minimum pH reached is around 4.2. This could be due either to substrate depletion or product inhibition. In this
 118 experiment, lactose is known to be in excess. Therefore, product, namely lactic acid, inhibition is assumed and should
 119 be considered while developing the model. For these initial conditions, results from both runs are in agreement. It also
 120 shows a pH difference in the order of 0.1 between the three samples from the same run.

121 Figure 4 shows the results of the 48 experiments. Each curve is similar to the one in Figure 3: time varies on the
 122 x-axis between 0 and 20 hours, and pH varies on the y-axis between a minimum of 4.2 and a maximum of 6.6. Each
 123 column represents an initial phage titer in PFU/mL, and each line represents an initial bacteria concentration in g/100L.
 124 In the first column, no phages are added to the milk. As the initial concentration of bacteria decreases, acidification is
 125 delayed, but the same final pH is reached.

126 Curves in Figure 4 can be divided into three distinct zones. The blue zone represents successful acidification, the
 127 final pH reached for all replicates is lower than 4.5. The gray zone represents the transition phase between success
 128 and failure. In this zone, the final pH is between 4.5 and 5.5. Finally, the red zone indicates the complete failure of
 129 acidification, all final pH values are higher than 5.5.

130 It can be seen in the transition zone that there are discrepancies between the final pH values and the curve shapes
 131 between replicates of the same repetition. For each set of initial conditions, the standard deviation between pH
 132 measurements at each time was calculated (i) separately for the 3 replicates of each run and (ii) including the 6
 133 measurements from both runs. Then, the conditions were grouped based on the final outcome: success, transition,
 134 and failure, and the standard deviations were averaged by zone.

135 The results are represented in Table 1. The standard deviations are higher in the transition zone compared to the success
 136 and failure zones for both runs, indicating more variability in the transition zone. This can be due to various possible
 137 factors such as experimental variabilities on the initial conditions or lack of homogeneity within the samples. It suggests
 138 a high sensitivity of the phenomena on initial conditions. Modeling should be used to quantify the behaviors in the

139 transition zone. In some cases, a slight increase in pH is observed such as for the initial conditions $X_{s0} = 10$ g/100L
 140 and $P_0 = 1.6 \times 10^5$ PFU/mL. It is thought to be linked to the release of amino acids from lysed bacteria making the
 141 milk more alkaline.

142 4. Model Development

143 The model consists of 5 ordinary differential equations with 11 parameters (θ). The susceptible (X_s) and infected
 144 (X_i) bacteria, lactose (L), and lactate concentrations (A_H), and phage titer (P) are grouped in a vector of state variables
 145 $X(t, \theta)$, which is a solution of the set of ordinary nonlinear differential equations:

$$\frac{dX}{dt} = f(t, X, \theta), \quad (1)$$

146 where $\theta \in \Theta$ is the vector of model parameters and Θ is the feasible parameter space. The pH is the only observable
 147 of the experiments, and is denoted as y , such that:

$$y = g(X), \quad (2)$$

148 where $g(X)$ is a vector describing the relationship between lactic acid and pH and is further detailed in equations (10)
 149 and (11) in Appendix A. The optimal set of parameters $\hat{\theta}$ was estimated using the least squares method. This was done
 150 using Python version 3.8 and the `least_squares` function from the `scipy.optimize` subpackage, version 1.10.1.
 151 The function was given another function that computes the vector of residuals between the experimental and simulated
 152 calibration data. Other arguments were left to default, such as `method="trf"` for the Trust Region Reflective algorithm
 153 (Branch et al. (1999)), the tolerance for termination by the change of the cost function `ftol=1e-8`, and tolerance for
 154 termination by the change of the independent variable `xtol=1e-8`.

155 Figure 5 is a graphical representation of the model. Table 2 shows the symbols of state variables and parameters.
 156 Detailed description of considered phenomena and model equations are given next.

157 4.1. Bacterial Concentrations

158 The growth of susceptible LAB (not yet infected by phages) was assumed to follow Monod-like growth kinetics
 159 (Monod, 1949). In milk fermentation, the substrate, i.e., lactose, limits bacterial growth in the Monod growth law,
 160 hence the presence of the half-saturation constant parameter K_L (Equation 4). The Monod half-saturation constant K_L
 161 is the substrate concentration at which the growth rate μ is half of the value of $\mu_{\max} \frac{L}{K_L+L}$. Growth is also inhibited
 162 by the product, namely lactic acid. We adopted the model of Luong (1985) to represent this inhibition. In addition,
 163 when bacteria are first put in a particular environment, they need an initial period to adapt. We adopted a modified

164 form (García et al., 2017) of Baranyi's model (Baranyi and Roberts, 1994) to represent this lag term (Equation 4).
 165 When phages are present, they attack bacteria by first being adsorbed on their surface, as shown in Figure 1. This was
 166 represented in Equation 3, where the adsorption term is a product of the concentration of susceptible bacteria, the
 167 phage titer, and the average adsorption rate k_A . Thus, the dynamics of bacterial growth and growth rate are represented
 168 by Equations 3 and 4, respectively:

$$\frac{dX_s}{dt} = \mu X_s - k_A X_s P \quad (3)$$

$$\mu = \mu_{\max} \frac{L}{L + K_L} \cdot \frac{a_0}{a_0 + (1 - a_0)e^{-\mu_{\max} t}} \left(1 - \left(\frac{A_H}{A_{H_{\max}}} \right)^\gamma \right) \quad (4)$$

169 Susceptible bacteria (X_s) attacked by phages become infected bacteria (X_i) and subsequently die with a specific lysis
 170 rate λ . Equation 5 describes the dynamics of infected bacteria:

$$\frac{dX_i}{dt} = k_A X_s P - \lambda X_i \quad (5)$$

171 4.2. Lactose metabolism to Lactic Acid

172 The dynamics of consumption of lactose and production of lactic acid are assumed to be proportional to the growth
 173 of bacteria. Yield coefficients of substrate consumption per biomass produced ($Y_{L/X}$) and product formation per
 174 substrate consumed ($Y_{A_H/L}$) are the proportionality factors. In the case of phage attack, infected bacteria are considered
 175 to compete with susceptible bacteria for substrate consumption (Santos et al., 2014). The dynamics of lactose utilization
 176 and lactic acid production are represented by Equations 6 and 7, respectively:

$$\frac{dL}{dt} = -Y_{L/X} \mu (X_s + X_i) \quad (6)$$

$$\frac{dA_H}{dt} = Y_{A_H/L} Y_{L/X} \mu (X_s + X_i) \quad (7)$$

177 4.3. Phage Infection

178 Phage multiplication is assumed to be proportional to the lysis of infected bacteria with β , the burst size, as the
 179 proportionality coefficient. Phages are removed from the medium when adsorbed. Phage deactivation is neglected
 180 because the experiments occur for a relatively short time. Equation 8 describes the evolution of phage titer:

$$\frac{dP}{dt} = -\alpha k_A X_s P + \beta \lambda X_i \quad (8)$$

4.4. Calibration and analysis of model subparts

Initially, model parameters were chosen based on the literature and expert knowledge. Then, the model was optimized by running a two-step optimization: first, an estimation of non-phage-related parameters, and then the estimation of the remaining parameters. The estimations were done by minimizing the sum of discrepancies between the experimental and simulated data, and the optimal set of parameters $\hat{\theta}$ was computed. The simulated pH was deduced from lactic acid concentration using the relation described in the Appendix A. Experimental data was divided into calibration data to estimate the parameters and validation data to independently assess model performance in a checkerboard pattern with respect to Figure 4 (if both the column and row numbers were even or odd, the initial condition was part of the validation data, otherwise it was part of the calibration data).

To begin with, a sub-model without phages was considered. Equations 5 and 8 were not taken into account and the phage adsorption term in Equation 3 was omitted. Among the 7 non-phage related parameters listed in Table 1, 2 parameters were fixed as follows. The yield coefficients $Y_{L/X}$ and $Y_{A_H/L}$ were highly correlated and could not be individually identified with the available data. $Y_{A_H/L}$ was fixed to a value of $0.8 \text{ (g/L).(g/L)}^{-1}$ that is commonly found in the literature ((Cachon and Divies, 1994), (Parente et al., 1994)). The substrate, lactose, was not limiting. The parameter K_L was then fixed to 0.5 g/L (Zacharof and Lovitt (2013)). Once the remaining 5 non-phage-related parameters of the sub-model were estimated, they were fixed, and the 4 phage-related parameters listed in Table 1 were estimated.

The initial conditions of phage titer and bacterial concentration were set as shown in Figure 4. The milk had an initial lactose concentration of 46 g/L . The initial lactic acid concentration was considered to be negligible. No infected bacteria were present at the beginning of the experiment.

4.5. Sensitivity analysis

To better understand the role of each phenomenon on the acidification dynamics, the sensitivity of final pH with respect to model parameters was computed for different initial conditions. The relative sensitivity of pH with respect to a parameter p was computed using Equation 9 from Cacuci et al. (2005):

$$\text{relative sensitivity} = \left(\frac{pH_{\text{up}} - pH_{\text{down}}}{pH} \right) \bigg/ \left(\frac{p_{\text{up}} - p_{\text{down}}}{p} \right) \quad (9)$$

205 where p_{down} and p_{up} are the values of the parameter decreased and increased by 5 % respectively, and pH_{down} and
 206 pH_{up} are the values of final pH for p_{down} and p_{up} , respectively. A variation of 5% was selected to minimize potential
 207 numerical issues and to ensure that the observed variation was due to the parameter change rather than numerical noise.
 208 A similar analysis was done with 1% change in parameters, and the results were consistent with those obtained using
 209 a 5% change.

210 5. Calibration, Validation, and Discussion

211 5.1. Parameter Estimation

212 The optimal set of parameters $\hat{\theta}$ was estimated. The relative standard deviation (RSD) of each parameter was
 213 calculated. Table 3 summarizes the values of these parameters, their units, and their RSD.

214 The RSD was less than 2 % for all estimated parameters. In general, parameter values estimated were within the
 215 ranges of values found in the literature. However, the values of the parameters vary depending on the specific strain,
 216 environmental conditions, and other factors.

217 For *Lactococcus lactis*, μ_{max} values in other studies range from 0.2 to 1.2 h⁻¹ (Parente et al., 1994; Boonmee et al.,
 218 2003; Zacharof and Lovitt, 2013; Chen et al., 2015). The value found using our model is within the same order of
 219 magnitude as values in the literature. The value of μ_{max} depends on the specific strain, the culture medium, and the
 220 conditions in which the bacteria are grown. Parente et al. (1994) and Zacharof and Lovitt (2013) found a yield of *L.*
 221 *lactis* growth over lactose consumption (Y_{L/X_s}) ranging from 0.04 to 0.09 g.(g/100L)⁻¹, which is close to our value.
 222 Cachon and Divies (1994) found a maximum lactic acid concentration ($A_{H_{\text{max}}}$) at uncontrolled pH of 9 g/L which is
 223 again compatible with our value. Lactoccal phages' burst size (β) values range between 10 and 250 particles per cell
 224 (Müller-Merbach et al., 2007), i.e. 10 to 250×10⁵(PFU/mL).(g/100L)⁻¹. The cell lysis rate (λ) is comparable to the
 225 inverse latency time between cell infection and burst. On average, phages have a latency period of 40 to 60 minutes
 226 (Müller-Merbach et al., 2007). Therefore, λ takes values between 1 and 1.5 h⁻¹. The adsorption rate k_A could not be
 227 compared to literature values due to unit incompatibility. The parameter a_0 can take values from 0 to 1 (García et al.,
 228 2017). The estimated value of 0.01 means that at the beginning of the fermentation, the growth is slow.

229 5.2. Model Validation

230 Figure 4 shows the model and the experimental data for pH for all 48 conditions. Globally, the model captured the
 231 major phenomena and mechanisms observed. It accurately delineated the three colored zones: acidification success,
 232 failure, and transition. It correctly predicted the shape of the curves in the blue (success) zone. There was high variability
 233 between the experimental acidifications in the gray (transition) zone. However, the model mostly fell between the

different experimental curves. Finally, the model predicted no acidification in the red (failure) zone. No mechanism to explain pH increase was included in the model, and no pH increase was predicted, as expected.

Besides pH , the model predicted the dynamics of the state variables: susceptible and infected LAB, lactose, lactic acid, and phage. As an example, Figure 6 shows the predicted dynamics of these variables, and susceptible bacteria's growth, for the case with an initial LAB concentration of 80 g/100L and an initial phage titer of 10^4 PFU/mL. Susceptible LAB grew to reach a maximum value of 180 g/100L, and when phages took over, their concentration decreased to become almost null towards the end of the experiment. In parallel, the concentration of infected LAB increased mostly after the susceptible bacteria's peak. Initially, phage titer decreased quickly due to adsorption on susceptible bacteria. It then increased due to phage burst by cell lysis. When the susceptible bacteria's concentration became null, the phage titer remained constant since no phage death mechanism was considered. At the end of the experiment, around 12 g/L of lactose were consumed and 9.5 g/L of lactic acid were produced. Susceptible bacteria's growth initially increased slowly due to the latency factor. It then increased rapidly until it reached a peak at 2.5 hours, after which it decreased due to lactic acid inhibition. Its largest value ($\simeq 0.3 \text{ h}^{-1}$) never approached $\mu_{\max} = 1.88 \text{ h}^{-1}$ (Table 3), confirming that the significance of parameters (here, μ_{\max}) is model-dependent.

5.3. Model use to assess acidification in case of phage attack

The final pH reached is considered a good indicator of the success or failure of mild acidification. The initial pH of milk is typically around 6.6. In the absence of phages, the final pH reached is 4.3, as acidification stops due to acid inhibition. In the case of phage attack, milk acidification can still be considered successful when the final pH is between 4.3 and 5.0. If the final pH is between 5.0 and 6.0, this is the transition zone between normal and no acidification. Finally, a final pH above 6.0 indicates failure of milk acidification due to phage attack.

Several simulations of the developed model were run, with different combinations of initial LAB concentrations and phage titers in the ranges of [10,80] (g/100L) and [10^4 , 10^7] (PFU/mL), respectively, where the model was validated. Figure 7a represents the final pH simulated using the model as a function of the initial conditions of bacteria and phages.

This experiment is a simplified real-life milk acidification experiment, where only one LAB strain and one phage interact. In such a case, if the initial concentration of LAB in the milk is known and if the phage contamination can be assessed, this graph can be used to predict the success or failure of acidification. If the final pH falls in the blue zone, it is safe to continue the cheese-making process. If it falls in the transition zone, which has been seen to be highly sensitive to the variability in initial conditions, special attention should be given to ensure that milk acidification will occur. However, if the pH falls in the red zone, it is advisable to stop the production process and clean the platform.

264 It can be seen in Figure 4 that there are discrepancies between the different replicates having theoretically the
 265 same initial conditions. This is most obvious in the transition (gray) zone. These discrepancies might be justifiable if
 266 small variations in the initial conditions have a large impact on the change of pH over time. To assess this hypothesis,
 267 the calibrated model was used to study the sensitivity of the final pH to the initial phage titer. Figure 7b shows the
 268 sensitivity analysis results. The model is clearly most sensitive in the transition zone. For example, for the initial
 269 conditions $X_{s0} = 10$ g/100L and $P_0 = 8 \times 10^4$ PFU/mL, the relative sensitivity of final pH to P_0 is 0.125. In this case,
 270 the model predicts a final pH of 5. A change of +50% and -50% in P_0 (likely to happen experimentally) leads to a
 271 final pH of 5.6 and 4.3, respectively, which is congruent with the experimental values. This high sensitivity supports
 272 the explanation of the observed experimental variability in the transition zone as being due to the initial phage titer
 273 variability. However, this variation could also be due to other factors, such as differences in the interaction between
 274 phages and bacteria. In the transition zone, the infection might be subject to biological variability, allowing bacteria in
 275 some repetitions/runs to escape the phages while others do not.

276 5.4. Sensitivity analysis of model parameters

277 Sensitivity analyses were performed to understand the dynamics of phage attack and the phenomena that govern
 278 it. Sensitivities of final pH (after 20 hours) to model parameters were computed for five different initial conditions
 279 marked in Figure 4: one in the success zone (a), three in the transition zone (b1, b2, and b3), and one in the failure zone
 280 (c). Figure 8 shows the results grouped per parameter. A positive value of relative sensitivity indicates that an increase
 281 in a parameter results in a corresponding increase in the final pH , whereas a negative value implies that an increase in
 282 a parameter leads to a decrease in the final pH .

283 For condition (a) in the success zone, the final pH was mostly sensitive to $A_{H_{max}}$. This result is to be expected as
 284 the reason behind acidification halting in this zone is acid inhibition and is not related to the presence of phages. The
 285 effect of acid inhibition was reduced in the transition and failure zones.

286 In the transition zone (for conditions (b1), (b2) and (b3)), four parameters (μ_{max} , α , β , and λ) have the highest
 287 impacts. An increased growth rate (higher μ_{max}) led to more lactose being metabolized to lactic acid by susceptible
 288 bacteria, reducing pH . Parameter α represents the number of phages disappearing as they get adsorbed on a bacterial
 289 cell, whether they infect it or not. A higher α means more infectious phages are disappearing, slowing the infection
 290 down. Parameter β , burst size, represents the number of phages released after cell lysis. As this burst size increases,
 291 more bacteria-infecting phages are released, which accelerates infection and increases the final pH . The parameter λ
 292 plays a role in two phenomena. On the one hand, an increase in the rate of cell lysis results in the faster elimination
 293 of infected cells that produce lactic acid, ultimately leading to a higher final pH . On the other hand, a higher cell lysis

294 rate leads to a quicker release of phages, targeting more susceptible bacteria and stopping lactic acid production which
295 also results in a higher final pH .

296 For condition (c), i.e., in the failure zone, the sensitivities of the final pH to model parameters were very small or
297 null. A higher μ_{\max} (an increased growth), or a smaller λ (a slower cell lysis), led to a lower final pH .

298 This analysis gives guidelines to shift the transition zone while expanding the success zone and reducing the failure
299 zone. Based on this model, adsorption kinetics (k_A) have shown to be much less important than burst size (β) and lysis
300 rate (λ) under selected initial conditions. In conclusion, phage-resistant LAB should be selected accordingly.

301 **5.5. Model limitations and future developments**

302 Although the kinetic model developed in this study was able to properly predict the outcome of a number of
303 contamination scenarios, and provide insights into process parameters and strain selection strategies, it has important
304 limitations that should be considered when interpreting the results. First, as any unstructured kinetic model built
305 from ordinary differential equations, it assumes that the tank where the milk acidification occurs is well mixed,
306 and no concentration gradients exist across it. This may not hold true in the case of our experimental setup, where
307 sedimentation of bacteria has occasionally been observed. This is also not the case in cheese production, as mixing is
308 only done at the beginning of the process, whereas most of the fermentation occurs in a solid matrix where there is
309 inherently uneven nutrient distribution. Secondly, we assume Monod-like kinetics for growth, where the main variables
310 controlling growth are the concentrations of the substrate (lactose) and the product (lactate). However, other variables
311 that play an important role on determining the growth rate, such as metabolic bottlenecks, temperature, osmotic
312 pressure, and other limiting nutrients (e.g., casein peptides), are not accounted for; this is especially relevant in large-
313 scale fermentations where some of these parameters do not remain constant. Finally, the developed model represents
314 the attack of a single type of phage on a single bacterial strain. This is normally not the case in cheese-making, where
315 often multiple types of phages can infect a microbial culture containing a community of different strains. A model
316 that would allow for multiple types of phages and bacteria should be expected to behave differently from the model
317 developed in this study, as not only it would simulate how the different phages interact with the different bacteria, but
318 also how different phages compete for the same bacterial strain, and how different bacteria interact among each other.

319 Going forward, it is possible to extend our method to quantify the impact of temperature, milk composition,
320 and additives such as rennet, on the dynamics of phage-host interactions. Moreover, this setup has the potential to
321 characterize new host-phage systems in an inexpensive and fast manner. Done systematically and at large scale, such
322 characterization may be used to classify many phage-host pairs to provide new insights about general phage virulence.
323 In addition, the use of non-invasive methods such as spectrophotometry, could also help quantify more state variables,
324 which would provide the foundation for even more advanced models of phage-host dynamics. Combined with modern

325 molecular biology and bioinformatics tools, it may even be possible to identify biomarkers in the host and phage that
 326 predicts phage virulence. Such biomarkers could be used to select more resilient strains for the dairy industry. We
 327 expect the model developed in this study to play a significant role in designing strategies for mitigating phage attacks,
 328 at the strain, community, and application levels. At the strain level, sensitivity analysis can identify which aspects of
 329 phage-host interactions should be addressed to make more robust strains. At the microbial community level, once this
 330 model is extended to account for other strains, it should be possible to find a blend of strains that minimize the risk of
 331 failure on the culture level if one or more strains are hit by phages. Finally, at the application level, the model can be
 332 used to devise strategies that mitigate the risk of fermentation failure in successive fillings, such as increasing rinsing
 333 (i.e. reducing the amount of phage left in the vat), late inoculation (i.e. after re-filling the tank with fresh milk), or
 334 reducing fermentation time (to limit phage build-up). These model-driven strategies can result in significant saving for
 335 the cheese-making industry.

336 6. Conclusion

337 This study contributes to the development and validation of dynamic phage attack models. We used a high
 338 throughput method to systematically create many inhibition trials in microtiter plates of different combinations of
 339 a host and its phage. Our model was validated on a broad range of initial conditions, and the experimental dataset
 340 included many replicates. Previous models have not been validated with such an extensive dataset, making our
 341 approach unique. The results were used to estimate bacteria- and phage-related parameters, such as specific growth
 342 rate, adsorption rate, latency time, and burst size, by fitting our model predictions to milk acidification curves.

343 This setup offers a fast and cost-effective method to characterize new host-phage systems. By integrating this
 344 model with molecular biology and bioinformatics tools, it could guide the selection of more resilient strains in the
 345 dairy industry. The model also provides strategies to mitigate phage attacks that could result in significant savings for
 346 cheese-making by reducing the risk of fermentation failure.

348 A. Appendix: Lactic Acid to pH calibration curve

349 In this study, pH is the only experimentally measured output. In order to link pH to lactic acid concentration, a
 350 state variable of the model, a direct ion equilibrium-based relation is not possible, because of the pH-dependent buffer
 351 effect of milk. Instead, a lactic acid titration in milk was generated and the data was fitted to a model proposed by
 352 Vereecken and Van Impe (2002):

$$Z = A_H - \frac{b_1}{2(b_1 - c_1)} \left[(A_H + b_1) - \sqrt{(A_H + b_1)^2 - 4(b_1 - c_1)A_H} \right] \quad (10)$$

$$pH = \frac{1}{2c_2} \left[A(b_2 - 2c_2)Z - \sqrt{A^2b_2^2Z^2 + 4Ac_2b_2^2Z} \right] + pH_{ini} \quad (11)$$

353 where Z is an intermediate variable and A_H is the concentration of total dissociated and undissociated lactic acid
 354 in mmol/L. Graphical interpretation of parameters A , b_1 , b_2 , c_1 , and c_2 can be found in Vereecken and Van Impe
 355 (2002). Table 4 shows the values of the estimated parameters from equations 10 and 11. Once the parameters were
 356 determined, they remained unchanged throughout the rest of the study. Squared average deviation was chosen as a
 357 measurement of the goodness of fit. It represents the square root of the average of squared differences between simulated
 358 and experimental data. Its value was 0.03 pH units. Figure 9 shows the fitting of the model equations to experimental
 359 data.

360 To acquire the data, increasing amounts of lactic acid were added to B-milk until a pH of approximately 4.0 was
 361 reached. Milk was placed at room temperature for 3 hours. Then, 100mL of milk was transferred to a beaker, where
 362 it was stirred with a magnetic stirrer for the duration of the experiment. The pH-meter was calibrated before use.
 363 Using a 10% solution of lactic acid, pH was stepwise decreased starting with 100 μ L intervals of added acid. When an
 364 increasing buffering activity was observed, the interval of added acid was adjusted conveniently. The pH was measured
 365 and plotted in relationship to the amount of added acids.

366 Declaration of competing interest

367 Benjamín José Sánchez, Ahmad A. Zeidan, and Jannik Vindeloev were employed by Chr. Hansen A/S, a global
 368 supplier of bacterial cultures for the dairy industry, at the time of writing this manuscript. The authors' views presented
 369 in this manuscript, however, are solely based on scientific grounds and do not reflect the commercial interests of their
 370 employer.

371 Data availability

372 Experimental Acidification data can be found here: <https://doi.org/10.57745/W3ZDG2> .

373 Acknowledgements

374 This paper is based on the experimental data of acidification curves obtained by the method developed and
 375 optimized by Louise Gammeltoft, Mette Schultz, Bjørn Serritzlev, Josue Castro, and Jeorgos Trihaas from Chr. Hansen
 376 A/S, Hørsholm, Denmark. We are grateful for their expertise and assistance in this project. In addition we would like
 377 to thank Ditte Ellegaard Christiansen for preparing the phages, Maiken Bjerrum for preparing the milk titration, and
 378 Thomas Janzen for the selection of phages and discussions.

379 **Funding**

380 This work is part of the E-MUSE project which was funded by the European Union's Horizon 2020 research and
 381 innovation programme under the Marie Skłodowska-Curie grant agreement N° 956126.

382 **Credit author statement**

383 **Michèle Bou Habib:** Conceptualization, Software, Formal Analysis, Methodology, Validation, Writing original
 384 draft. **Emmanuel Bernueau:** Conceptualization, Software, Formal analysis, Methodology, Review & Editing. **Ioan-**
 385 **Cristian Trelea:** Conceptualization, Formal analysis, Methodology, Review & Editing. **Benjamín-José Sánchez:**
 386 Conceptualization, Formal Analysis, Methodology, Review & Editing. **Dominique Swennen:** Conceptualization,
 387 Funding acquisition, Review & Editing. **Ahmad Zeidan:** Funding acquisition, Review & Editing. **Jannik Vindeloev:**
 388 Conceptualization, Data curation, Methodology, Review & Editing.

389 **References**

- 390 Baranyi, J., Roberts, T.A., 1994. A dynamic approach to predicting bacterial growth in food. *International journal of food microbiology* 23, 277–294.
- 391 Beretta, E., Kuang, Y., 1998. Modeling and analysis of a marine bacteriophage infection. *Mathematical biosciences* 149, 57–76.
- 392 Boonmee, M., Leksawasdi, N., Bridge, W., Rogers, P.L., 2003. Batch and continuous culture of *Lactococcus lactis* nz133: experimental data and
 393 model development. *Biochemical engineering journal* 14, 127–135.
- 394 Branch, M.A., Coleman, T.F., Li, Y., 1999. A subspace, interior, and conjugate gradient method for large-scale bound-constrained minimization
 395 problems. *SIAM Journal on Scientific Computing* 21, 1–23.
- 396 Brüssow, H., 2001. Phages of dairy bacteria. *Annual Reviews in Microbiology* 55, 283–303.
- 397 Bull, J., Millstein, J., Orcutt, J., Wichman, H., 2006. Evolutionary feedback mediated through population density, illustrated with viruses in
 398 chemostats. *The American Naturalist* 167, E39–E51.
- 399 Cachon, R., Divies, C., 1994. Generalized model of the effect of pH on lactate fermentation and citrate bioconversion in *Lactococcus lactis* ssp. *lactis*
 400 biovar. *diacetylactis*. *Applied microbiology and biotechnology* 41, 694–699.
- 401 Cacuci, D.G., Ionescu-Bujor, M., Navon, I.M., 2005. Sensitivity and uncertainty analysis, volume II: applications to large-scale systems. CRC
 402 press.
- 403 Cairns, B.J., Timms, A.R., Jansen, V.A., Connerton, I.F., Payne, R.J., 2009. Quantitative models of in vitro bacteriophage–host dynamics and their
 404 application to phage therapy. *PLoS Pathogens* 5, e1000253.
- 405 Campbell, A., 1961. Conditions for the existence of bacteriophage. *Evolution* , 153–165.
- 406 Chaudhry, W.N., Pleška, M., Shah, N.N., Weiss, H., McCall, I.C., Meyer, J.R., Gupta, A., Guet, C.C., Levin, B.R., 2018. Leaky resistance and the
 407 conditions for the existence of lytic bacteriophage. *PLoS biology* 16, e2005971.
- 408 Chen, J., Shen, J., Ingvar Hellgren, L., Ruhdal Jensen, P., Solem, C., 2015. Adaptation of *Lactococcus lactis* to high growth temperature leads to a
 409 dramatic increase in acidification rate. *Scientific reports* 5, 14199.
- 410 Fox, P.F., McSweeney, P.L., 2017. Cheese: an overview. *Cheese* , 5–21.

Predicting milk acidification

- 411 García, M.R., Cabo, M.L., Herrera, J.R., Ramilo-Fernández, G., Alonso, A.A., Balsa-Canto, E., 2017. Smart sensor to predict retail fresh fish quality
412 under ice storage. *Journal of food engineering* 197, 87–97.
- 413 Garneau, J.E., Moineau, S., 2011. Bacteriophages of lactic acid bacteria and their impact on milk fermentations. *Microbial cell factories* 10, 1–10.
- 414 Kongo, J.M., 2013. Lactic acid bacteria as starter-cultures for cheese processing: past, present and future developments. *Lactic acid bacteria-R &*
415 *D for food, health and livestock purposes* , 1–22.
- 416 Ledebøer, A., Bezemer, S., De Haard, J., Schaffers, I., Verrips, C., Van Vliet, C., Düsterhöft, E.M., Zoon, P., Moineau, S., Frenken, L., 2002.
417 Preventing phage lysis of *Lactococcus lactis* in cheese production using a neutralizing heavy-chain antibody fragment from llama. *Journal of*
418 *dairy science* 85, 1376–1382.
- 419 Lenski, R.E., Levin, B.R., 1985. Constraints on the coevolution of bacteria and virulent phage: a model, some experiments, and predictions for
420 natural communities. *The American Naturalist* 125, 585–602.
- 421 Levin, B.R., Stewart, F.M., Chao, L., 1977. Resource-limited growth, competition, and predation: a model and experimental studies with bacteria
422 and bacteriophage. *The American Naturalist* 111, 3–24.
- 423 Luong, J., 1985. Kinetics of ethanol inhibition in alcohol fermentation. *Biotechnology and bioengineering* 27, 280–285.
- 424 Mahony, J., Tremblay, D.M., Labrie, S.J., Moineau, S., van Sinderen, D., 2015. Investigating the requirement for calcium during lactococcal phage
425 infection. *International Journal of Food Microbiology* 201, 47–51.
- 426 Marcó, M.B., Moineau, S., Quiberoni, A., 2012. Bacteriophages and dairy fermentations. *Bacteriophage* 2, 149–158.
- 427 Moineau, S., Lèvesque, C., 2005. Control of bacteriophages in industrial fermentations. *Bacteriophages: biology and applications* , 285–296.
- 428 Monod, J., 1949. The growth of bacterial cultures. *Annual review of microbiology* 3, 371–394.
- 429 Müller-Merbach, M., Kohler, K., Hinrichs, J., 2007. Environmental factors for phage-induced fermentation problems: replication and adsorption of
430 the *Lactococcus lactis* phage p008 as influenced by temperature and pH. *Food microbiology* 24, 695–702.
- 431 Parente, E., Ricciardi, A., Addario, G., 1994. Influence of pH on growth and bacteriocin production by *Lactococcus lactis* subsp. *lactis* 14onwc during
432 batch fermentation. *Applied Microbiology and Biotechnology* 41, 388–394.
- 433 Poulsen, V.K., Derkx, P., Oregaard, G., 2019. High-throughput screening for texturing *Lactococcus* strains. *FEMS microbiology letters* 366, fnz001.
- 434 Santos, S.B., Carvalho, C., Azeredo, J., Ferreira, E.C., 2014. Population dynamics of a salmonella lytic phage and its host: implications of the host
435 bacterial growth rate in modelling. *PLoS one* 9, e102507.
- 436 Sinha, S., Grewal, R.K., Roy, S., 2020. Modeling phage–bacteria dynamics, in: *Immunoinformatics*. Springer, pp. 309–327.
- 437 Vereecken, K.M., Van Impe, J.F., 2002. Analysis and practical implementation of a model for combined growth and metabolite production of lactic
438 acid bacteria. *International Journal of Food Microbiology* 73, 239–250.
- 439 Zacharof, M.P., Lovitt, R.W., 2013. Modelling and simulation of cell growth dynamics, substrate consumption, and lactic acid production kinetics
440 of *Lactococcus lactis*. *Biotechnology and bioprocess engineering* 18, 52–64.

Predicting milk acidification

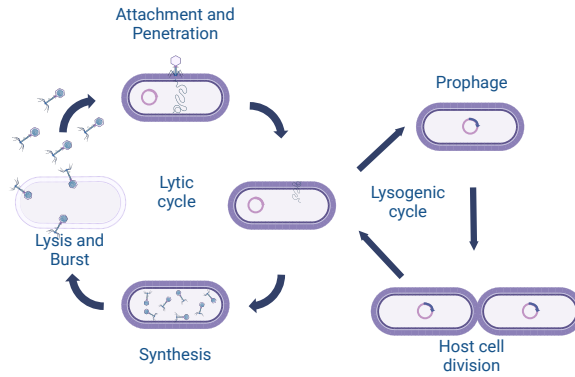


Figure 1: The lytic and lysogenic cycles of phage attack, after Sinha et al. (2020). Created with BioRender.com.

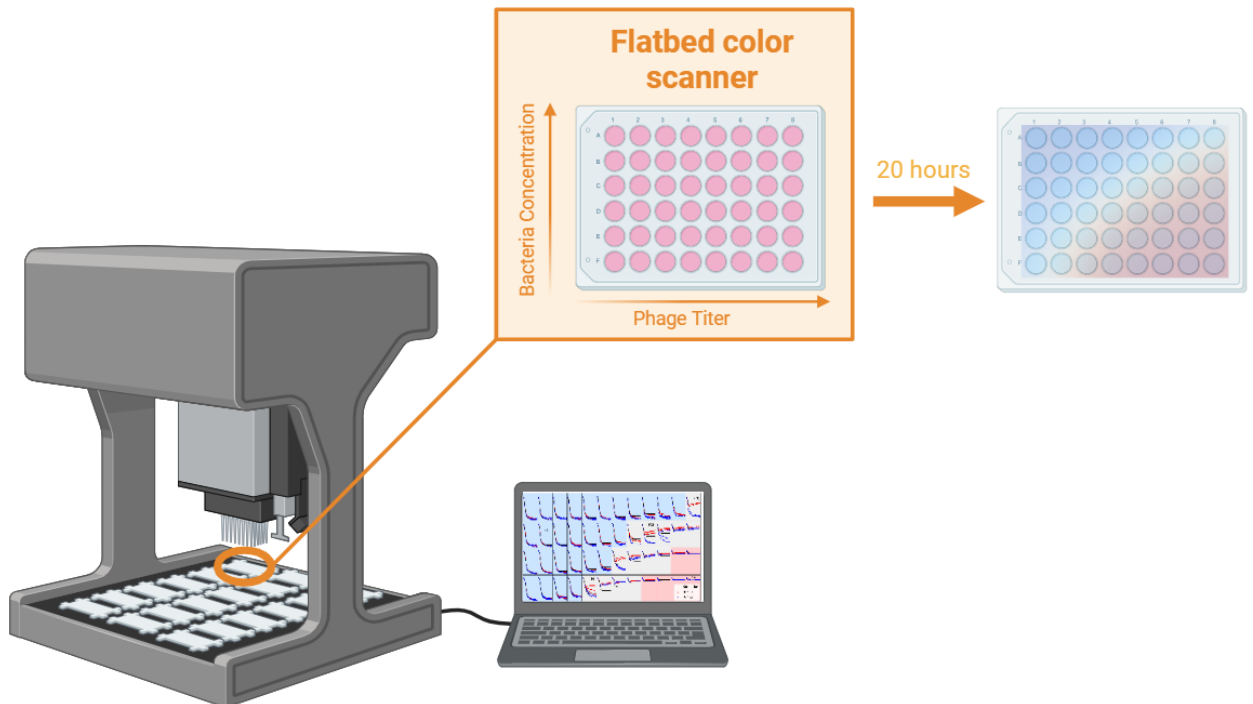


Figure 2: Conceptual diagram of the experiment. Acidification experiments were performed in a volume of 400L using deep 96-well plates, and a 2D concentration gradient of strain-to-phage. After inoculation of the sensitive strain and its phage, the plates were incubated for 20h on top of a flat-bed scanner at 30°C. *pH*-dependent changes in color were recorded every 4 min and converted into *pH*. Created with BioRender.com.

Predicting milk acidification

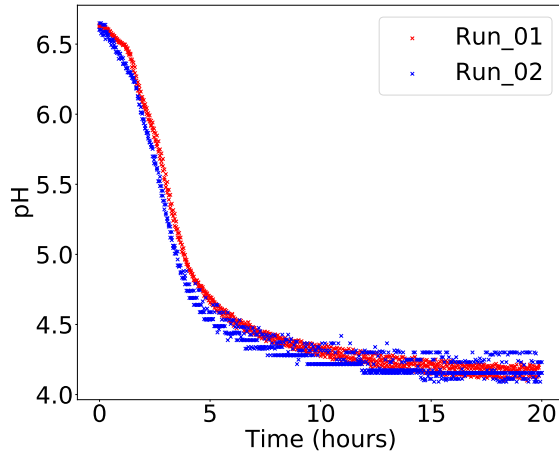


Figure 3: Acidification curves for $P_0 = 0$ PFU/mL and $X_{s0} = 40$ g/100L. Experiments were done in two separate runs 'Run_01' and 'Run_02', each with three repetitions.

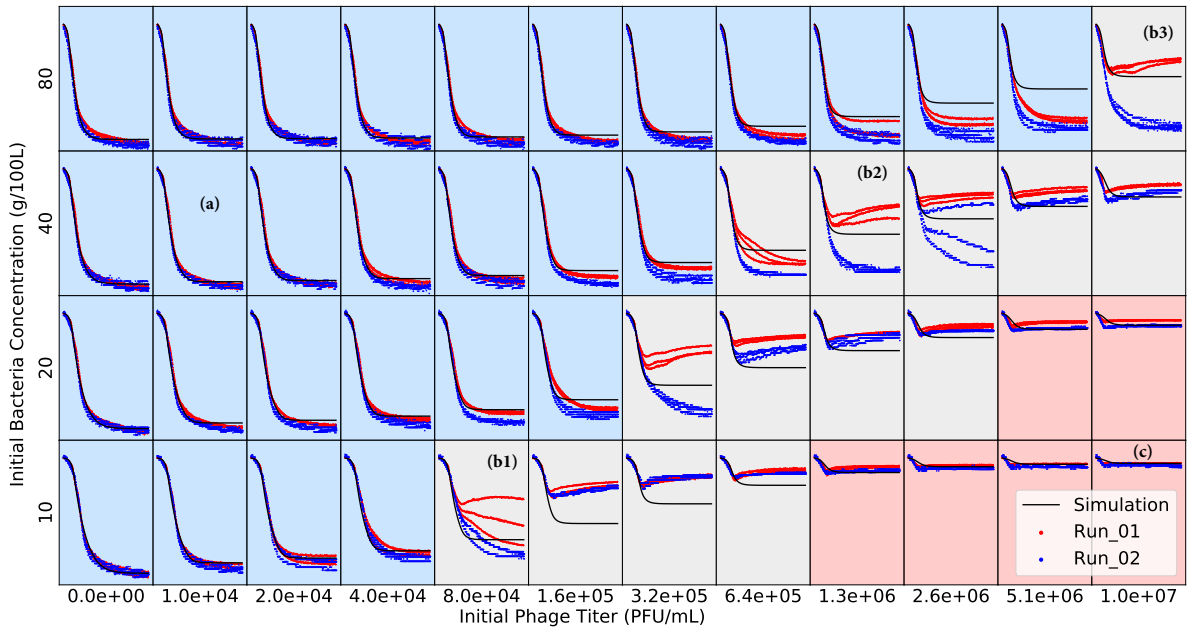


Figure 4: Acidification curves for all 48 conditions of phage titer and LAB concentration. Each curve has the same scale as Figure 3. The x-axis represents time, ranging from 0 to 20 hours, and the y-axis represents pH, ranging from 4 to 6.6. The black curve is the result of the model simulation after parameter fitting (section 4.4). a, b1, b2, b3, and c are chosen conditions for the sensitivity analysis in 5.4. Background: blue: success, gray: transition zone, red: failure.

	Success zone	Transition zone	Failure zone
Run_01	0.030	0.051	0.009
Run_02	0.038	0.055	0.013
Both Runs	0.065	0.186	0.039

Table 1

Values of the average standard deviations per zone. For each set of initial conditions, the standard deviation between pH measurements at each time was calculated (i) separately for the 3 replicates of each run and (ii) including the 6 measurements from both runs. Then, the conditions were grouped based on the final outcome: success, transition, and failure, and the standard deviations were averaged by zone.

Predicting milk acidification

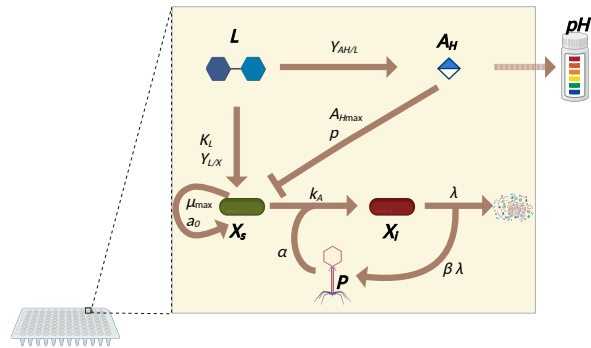


Figure 5: Graphical representation of the phage attack model. Symbols are all explained in Table 2. Created with BioRender.com.

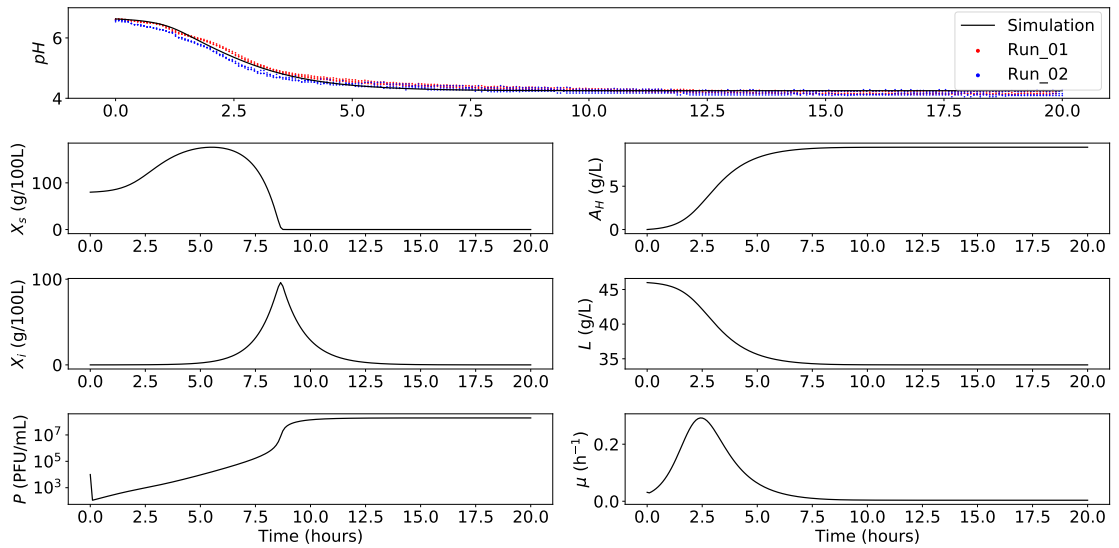
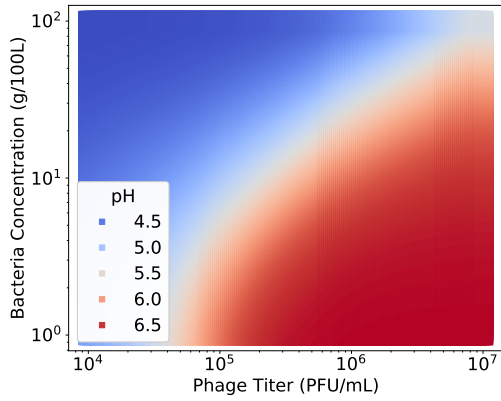
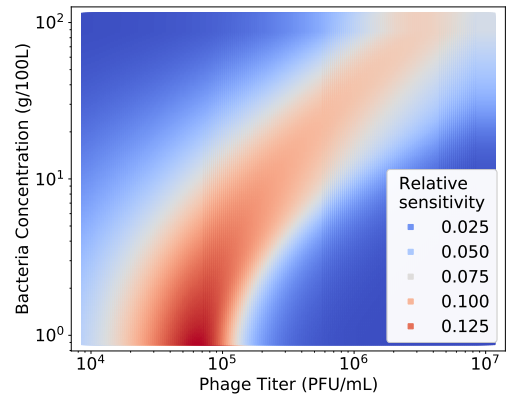


Figure 6: Model dynamics predictions for $X_{s0} = 80$ g/100L and $P_0 = 10^4$ PFU/mL

Predicting milk acidification



(a) Simulated final pH as a function of initial conditions



(b) Relative sensitivity on final pH on initial phage titer as a function of initial conditions

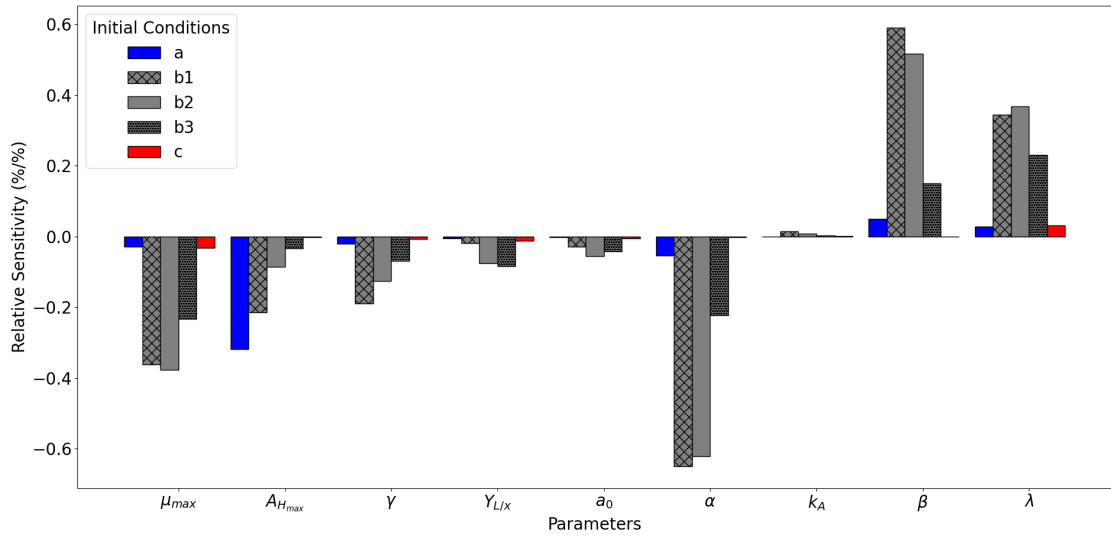


Figure 8: Final pH sensitivity to model parameters for 5 different initial conditions marked in Figure 4

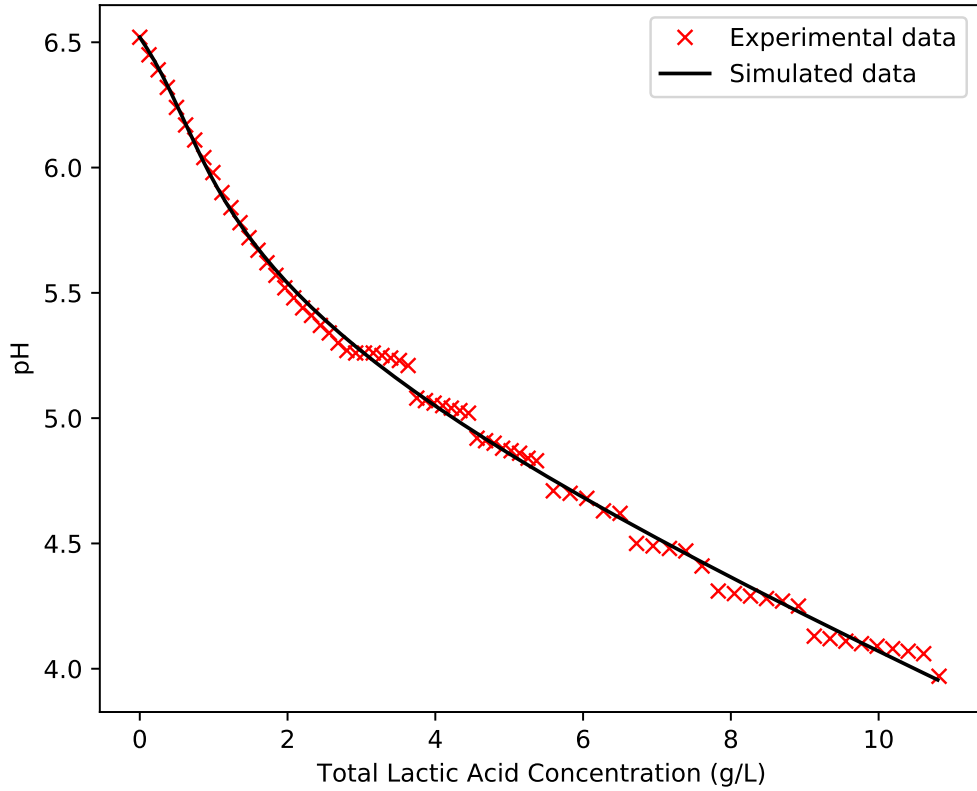


Figure 9: Conversion of total lactic acid to pH. The titration was done by adding 10% solution of lactic acid to standardized B-milk.

Category	Symbol	Definition	Unit
	t	Time	h
State Variables	A_H	Lactic Acid Concentration	g/L
	L	Lactose Concentration	g/L
	X_s	Susceptible Bacteria Concentration	g/100L
	X_i	Infected Bacteria Concentration	g/100L
	P	Phage Titer	PFU/mL
Non phage-related parameters	μ_{max}	Theoretical Maximal Growth Rate	h^{-1}
	$Y_{A_H/L}$	Yield of Product over Substrate	$(g/L).(g/L)^{-1}$
	$Y_{L/X}$	Yield of Substrate Consumption over Biomass Growth	$(g/L).(g/100L)^{-1}$
	γ	Shape Factor	-
	K_L	Half-saturation Constant	g/L
	$A_{H_{max}}$	Maximal Acid Concentration	g/L
	a_0	Lag Parameter	-
Phage-related parameters	α	Phage to Bacteria Ratio	$(PFU/mL).(g/100L)^{-1}$
	k_A	Adsorption Rate	$(PFU/mL)^{-1}.h^{-1}$
	β	Burst Size	$(PFU/mL).(g/100L)^{-1}$
	λ	Cell Lysis Rate	h^{-1}

Table 2

List of symbols for the phage attack model. State variables were initially set to experimental design initial conditions. Non-phage related parameters were estimated from acidification data with no phages, except for K_L and $Y_{A_H/L}$ which were fixed. Phage-related parameters were estimated from the rest of the acidification data.

Symbol	Definition	Value	Relative Standard Deviation (%)	Unit
μ_{\max}	Theoretical Maximal Growth Rate	1.88	0.42	h^{-1}
$Y_{A_H/L}$	Yield of Product over Substrate	0.80	Fixed according to literature value	$\text{g} \cdot (\text{g}/100\text{L})^{-1}$
$Y_{L/X}$	Yield of Substrate Consumption over Biomass Growth	0.10	1.27	$\text{g} \cdot (\text{g}/100\text{L})^{-1}$
γ	Shape Factor	0.24	0.58	-
K_L	Half-saturation Constant	0.50	as substrate is not limiting	g/L
$A_{H\max}$	Maximal Lactic Acid Concentration	9.58	0.03	g/L
a_0	Lag Parameter	0.01	1.53	-
α	Phage to Bacteria Ratio	8.79×10^5	0.18	$(\text{PFU}/\text{mL}) \cdot (\text{g}/100\text{L})^{-1}$
k_A	Adsorption Rate	2.73×10^{-6}	0.02	$(\text{PFU}/\text{mL})^{-1} \cdot \text{h}^{-1}$
β	Burst Size	18.90×10^5	0.35	$(\text{PFU}/\text{mL}) \cdot (\text{g}/100\text{L})^{-1}$
λ	Cell Lysis Rate	0.92	0.26	h^{-1}

Table 3

Parameter values and standard deviations after estimation. Parameters K_L and $Y_{A_H/L}$ were fixed.

Parameter	Estimated Value	Relative Standard Deviation (%)	Unit
A	0.01	1.22	$(\text{mmol}/\text{L})^{-1}$
b_1	8.12	1.34	mmol/L
c_1	1.07	7.08	mmol/L
b_2	1.59	1.93	unitless
c_2	0.29	6.08	unitless

Table 4

Estimation of parameters for Lactic Acid to pH conversion